Northern Arizona Ecological Conservation

Assessing Quaking Aspen Health in Northern Arizona Using Earth Observations

Summer 2025 | Pop-Up Project – Northern Arizona University
August 8th, 2025

Authors: Ikram Morso (Analytical Mechanics Associates), Luke Collins (Analytical Mechanics Associates), Margaret Cox (Analytical Mechanics Associates), Melissa Schwan (Analytical Mechanics Associates)

Abstract: Quaking aspen (*Populus tremuloides*) forests in Northern Arizona provide critical habitat for endangered bird species and support regional tourism and recreation. However, aspen populations are declining due to a combination of abiotic and biotic stressors. In response, land managers implemented strategies, such as ungulate exclusion fencing, prescribed burns, and stand thinning, but efforts are constrained by limited data on where and when to intervene. This project worked in collaboration with the U.S. Forest Service, the National Park Service, the Arizona Department of Forestry and Fire Management, and Northern Arizona University School of Forestry. The team utilized Earth observations (EOs) and geospatial analysis to assess long-term trends in aspen extent. We applied a random forest classification and phenological analysis using Landsat 8 Operational Land Imager (OLI) imagery (2014–2024), deriving the Normalized Difference Vegetation Index (NDVI), Normalized Difference Yellowness Index (NDYI), and Modified Normalized Difference Water Index (MNDWI). The team sourced elevation, slope, and aspect data from the U.S. Geological Survey's USGS Shutter Radar Topography Mission Digital Elevation Models (SRTM DEM). A 2017 aspen presence map was produced with an overall accuracy of 79.15%, classifying approximately 41.41 square miles of aspen forest. Time-series analysis of vegetation and climate indicators revealed an overall decrease in aspen extent between 2017 and 2024. These results provide partners with a scalable, repeatable tool to identify regeneration hotspots and inform restoration priorities. While our classification was limited by the availability of known aspen training data, this study demonstrated the feasibility of leveraging EOs to enhance field-based forest monitoring and decision-making.

Key Terms: Quaking Aspen, Coconino National Forest, Landsat 8 OLI, MODIS, Normalized Difference Vegetation Index (NDVI), Normalized Difference Yellow Index (NDYI), Random Forest, Modified Normalized Difference Water Index (MNDWI)

Advisors: Dr. Paul Arellano (Northern Arizona University), Dr. Alexander Shenkin (Northern Arizona University), Dr. Xia Cai (National Aeronautics and Space Administration)

Lead: Jane Zugarek (California – JPL)

1. Introduction

In the Southwestern United States, Arizona notably has approximately 18.6 million acres of forested land, which contain diverse ecosystems of ecological importance and serve as a major tourist attraction (Forestry, 2023). Quaking aspen (*Populus tremuloides*) is an iconic species in these landscapes, providing numerous ecosystem benefits, such as watershed protection, natural fuel break, critical animal habitat, and increased biodiversity (Crouch et al., 2025). Arizona alone has over 153,000 acres of documented aspen-dominated forests (Shaw et al., 2018); however, aspen populations across the western U.S. are declining due to a combination of biotic and abiotic stressors (Crouch et al., 2021; Crouch et al., 2025). Prolonged drought and rising temperatures associated with climate change have decreased the moisture availability necessary for successful aspen regeneration. Compounding this, chronic ungulate herbivory, particularly in areas lacking protective understory or recent low-severity fire, has further suppressed regeneration and led to the formation of aging stands with limited recruitment potential (Crouch et al., 2025). While wildfires can create conditions favorable for aspen regeneration by reducing conifer competition, the lack of sufficient post-fire precipitation and ongoing herbivory often limits recovery and increases the risk of erosion and conifer encroachment (Hamilton et al., 2009). In addition to these stressors, the invasive oystershell scale (*Lepidosaphes ulmi)* has emerged as a significant threat in the region. Oystershell scale insects attach to the trunks and branches of aspen trees and feed on the sap, reducing the moisture available to the tree and increasing its susceptibility to pathogens. When infestation becomes significant enough, it can kill the tree, with young aspen being more susceptible (Crouch et al., 2021). These threats to aspen collectively have prompted management interventions from multiple organizations with an interest in preserving the ecological and economic benefits provided by quaking aspen in northern Arizona.

For this project, we partnered with (1) the US Department of Agriculture, United States Forest Service (USFS), Coconino National Forest, Flagstaff Ranger District; (2) USFS Northern Research Station; (3) USFS Southwestern Region, Arizona Zone Forest Health; (4) USFS Coconino National Forest, Mogollon Rim Ranger District, (5) National Park Service (NPS), Wupatki, Sunset Crater Volcano, and Walnut Canyon National Monuments, (6) Arizona Department of Forestry and Fire Management, and (7) Northern Arizona University School of Forestry. These groups manage, research, and monitor quaking aspen stands in forests across northern Arizona and are concerned with widespread aspen die-off and low recruitment of young aspen into the population within their management areas. They aim to focus their limited resources on areas with the greatest potential for long-term aspen success. Partners have applied management strategies, such as (1) ungulate exclusion fences to prevent over-browsing on young aspen stems, (2) targeted thinning of encroaching conifers near aspen stands, (3) controlled burning of aspen stands to promote regrowth and control oystershell scale infestation, and (4) cutting infested aspen to prevent the oystershell scale insect from spreading. While these methods have been effective at the plot scale, monitoring aspens at the forest scale has been limited by workforce and logistical constraints. This study aimed to evaluate the feasibility of using Earth observations (EO) to detect and classify aspen and mixed aspen stands using vegetation indices and topographic data.

Aerial surveys conducted in May 2017 by USFS have aided in monitoring aspen health by documenting their distribution, levels of conifer encroachment, and signs of dieback (DePinte et al., 2018); however, this information is now outdated considering recent forest fires (Stoddard et al., 2024) and possible other factors. More recent ground surveys conducted between 2020 and 2023 provided insights into overstory and regeneration dynamics; however, the limited spatial coverage of these surveys constrains broader landscape-level assessments (Crouch et al., 2025). While both aerial and ground surveys offer detailed information, they lack the spatial extent and temporal frequency needed for large-scale monitoring. EOs help bridge this gap by enabling consistent, wide-area observation for forest health assessment and tree classification. Oukrop et al. (2011) demonstrated the use of high-resolution multispectral satellite imagery to identify aspen stands in southern Utah and Colorado. Additional studies have reported promising results using phenological approaches and remote sensing techniques to map aspen extent and assess health (Grigorieva et al., 2020; Oukrop et al., 2011; Sankey et al., 2011; Troshin et al., 2025).

The study area for this project is situated in northern Arizona (Figure 1), with project analysis focused primarily on the Coconino National Forest, hereafter referred to as Coconino, and its surrounding landscapes, as identified through in situ data provided by our partners. Covering approximately 1.856 million acres, Coconino spans a broad elevational range from 2,600 feet to 12,633 feet and contains strong elevation-related temperature and moisture gradients. Higher elevations are often cooler and have more moisture, conditions that favor quaking aspen stands (USDA, 2025). Our study period spanned 2014–2024, offering a meaningful window to observe patterns of increasing climate stress, herbivory pressure, and emerging pest threats that influenced aspen health and regeneration in northern Arizona. It also encompassed key disturbance events, such as the Museum Fire (2019) and the Pipeline Fire (2022), providing important context for assessing shifts in aspen extent over time.

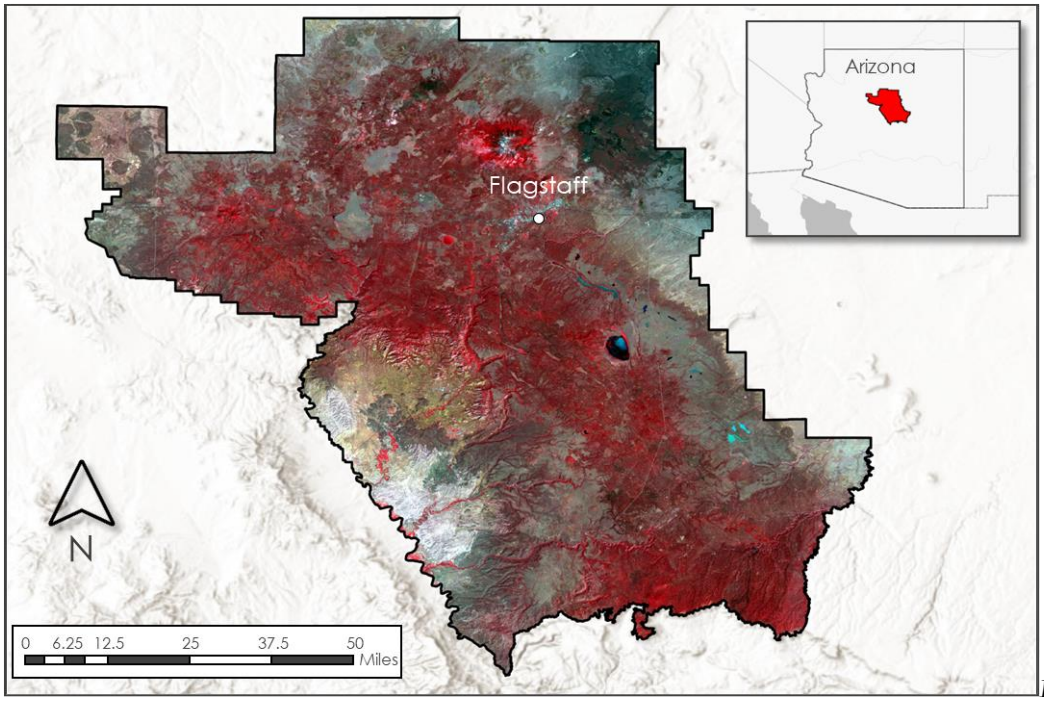

Figure 1. False color (NIR-Red-Green) composite image acquired by Landsat 8 OLI in October 2023, clipped to the boundaries of USFS Coconino and southern Kaibab National Forests, including the adjacent National Park Service units: Wupatki National Monument, Sunset Crater National Monument, and Walnut Canyon National Monument. This imagery showcases the diverse topography and land cover of northern Arizona, featuring forested plateaus, volcanic features, and extensive canyon systems.

2. Methodology

2.1 Data Acquisition

We collected data from EO platforms, gridded climate products, and partner-provided field datasets (Table 1). We used Google Earth Engine (GEE; Gorelick et al., 2017) to download Landsat 8 OLI imagery and Shuttle Radar Topography Mission (SRTM) Digital Elevation Models (DEM) and to generate raster predictor variables for the 2017 and 2024 classifications (Gorelick et al., 2017). We also generated input variables using Harmonized Landsat Sentinel-2 imagery for the 2024 classification, as the 2024 Landsat 8 images were sparse due to cloud cover. We obtained MODIS vegetation indices for 2014–2024 from GEE to assess seasonal vegetation dynamics. We also downloaded CHIRPS 2.0 daily precipitation data (Climate Hazards Center, 2014–2024) and Daymet daily temperature data (Funk et al., 2015; Thornton et al., 2021) through RStudio to characterize monsoon and temperature variability. Our partners provided a 2017 aerial mapping shapefile of aspen cover, from which we extracted training points for the 'Aspen' and 'Mixed Aspen' classes.

Table 1
Datasets

Data	Data Source	Parameter, resolution	Acquisition Method	Dates
Landsat 8 OLI/Level 2, Collection 2, Tier 1 (LS8)	USGS and NASA Earth Observing Systems	Multispectral bands, 30m	GEE	01/01/2014 – 12/31/2024
Sentinel-2 Multispectral Instrument (MSI)	NASA LP DAAC	Harmonized Landsat Sentinel-2 (HLS) Multispectral bands, 30m	GEE	01/01/2024 – 12/31/2024
Terra Moderate Resolution Imaging Spectroradiometer (MODIS)	NASA LP DAAC	Vegetation indices (NDVI), 250m	GEE	01/01/2014 – 12/31/2024
Climate Hazards Group Infared Precipitation with Station Data 2.0 (CHIRPS)	UCSB/CHG	Daily precipitation, 0.05° (~5km)	Downloaded from https://www.chc.ucsb.edu	01/01/2014 – 12/31/2024
Daymet	NASA ORNL DAAC at Oak Ridge National Laboratory	Daily temperature, 1km	RStudio	01/01/2014 – 12/31/2024
Global Ecosystem Dynamics Investigation (GEDI) Level 2A and 2B products	NASA GEDI / LP DAAC	Canopy height, 25m	RStudio	01/01/2024 – 12/31/2024
USGS Digital Elevation Model (DEM)	NASA SRTM / USGS	Elevation, ~30m	GEE	2015
National Land Cover Database (NLCD)	USGS / MRLC Consortium	Land Cover Classes 30 m	Downloaded from USGS MRLC	2017, 2024

2.2 Data Processing

2.2.1 Vegetation Indices

We analyzed Terra MODIS vegetation indices Normalized Difference Vegetation Index (NDVI) and Enhanced Vegetation Index (EVI) for 2014–2024 using GEE to identify the start, peak, and end of the vegetation growing season. This seasonality analysis guided phenological interpretation and informed the selection of optimal acquisition dates for Landsat 8 imagery used in our random forest model. We processed Landsat 8 imagery in GEE by applying a 20% cloud mask, converting to surface reflectance, and creating monthly median composite images. For each composite, we calculated NDVI using Equation 1 (Kriegler, F. et al., 1969), Normalized Difference Yellowness Index (NDYI) using Equation 2 (Sulik & Long, 2016), and Modified Normalized Difference Water Index (MNDWI) using Equation 3 (Xu, 2006). NDVI measures vegetation greenness and is related to photosynthetic activity, vegetation type, and density. NDYI captures autumn leaf yellowing by the end of the growing season each year. MNDWI provides information for assessing proximity to water sources, as water availability is an important abiotic factor influencing aspen regeneration. Cook et al. (2024) found that aspen stands generally exhibited higher MNDWI values in riparian and mountainous areas, suggesting that proximity to open water may contribute to regeneration potential in

those areas. We also calculated summary statistics, including the mean and standard deviation of each index and the Landsat bands, across all 12 monthly composites to capture intra-annual variability. We projected all imagery to a uniform Coordinate Reference System (CRS) (EPSG: 4326) and exported the products as GeoTIFFs for use in the Random Forest (RF) classification model. We calculated the same indices from the Harmonized Landsat Sentinel-2 bands, to include them in the 2024 RF model for aspen classification.

$$\text{NDVI} = \frac{\text{Red} - \text{NIR}}{\text{Red} + \text{NIR}} \tag{1}$$

$$\text{NDYI} = \frac{\text{Blue} - \text{Green}}{\text{Blue} + \text{Green}} \tag{2}$$

$$\text{MNDWI} = \frac{\text{Green} - \text{SWIR1}}{\text{Green} + \text{SWIR1}} \tag{3}$$

2.2.2 Climate & Topography

To assess seasonal and annual climate variability from 2014–2024, we processed CHIRPS 2.0 daily precipitation Network Common Data Form (NetCDF) files and Daymet v4 daily temperature data using RStudio and clipped them to the study area on a common 5 km grid. For precipitation, we extracted daily values, interpolated them to generate rasters showing spatial and annual changes, and calculated monthly totals saved as .csv tables for monsoon season analysis and dry year identification. For temperature, we generated annual raster images to visualize spatial differences and temporal changes and summarized daily values to monthly means, which we saved as .csv tables for the climate assessments of our area of interest. To compute topographic variables, we used a 30m SRTM DEM clipped to our study region for elevation and derived slope and aspect using GEE in conjunction with the mentioned DEM.

2.2.3 Random Forest Classification

We prepared training and testing datasets for the 2017 supervised RF classification model by integrating partner-provided aspen survey data with land cover classes from the 2017 NLCD. We defined five vegetation classes: Aspen, Mixed Aspen/Conifer, Conifer, Grassland, and Shrub. Using the 2017 aerial survey data, we selected polygons where conifer encroachment was classified as *very low* or *low* as Aspen polygons, while polygons with *moderate* encroachment formed the Mixed Aspen/Conifer class. We excluded polygons with *high* encroachment to avoid mislabeling. We generated Conifer polygons from the NLCD evergreen forest (class 42), incorporating expert knowledge from our partners to ensure they represented conifer monocultures. Grassland and Shrub classes were derived from the corresponding 2017 NLCD classes. To compute a classification map for 2024, we first removed any of the 2017 polygons with a difference (2024-2017) in NDVI less than -0.2 to be used as training data for the Aspen and Mixed Aspen/Conifer classes (Table A1). Due to the lack of quality data for from Landsat 8 data alone, we calculated all input vegetation indices (e.g., NDVI and NDYI) for 2024 from HLS data that includes both Landsat 8 and Sentinel-2 imagery. Grassland and Shrub classes were updated from the corresponding 2024 NLCD classes.

2.2.4 Tree Canopy Profile

We used the rGEDI (Silva et al., 2020) package in RStudio to download available GEDI Level 2A and 2B data for our study area in 2024. We accessed plant metrics available in the Hierarchical Data Format (HDF) 5 file types through the readLevel and getLevel functions (available in rGEDI) and converted them into a spatial point data frame, saved as a .csv and a shapefile, for each acquisition. These included the remotely sensed locations within the beam path and information on biophysical variables, including ground elevation, relative canopy height, and plant area index (PAI), a ratio of leaf and woody area to ground area.

2.3 Data Analysis

2.3.1. Climate Assessment

We analyzed seasonal and interannual climate variability from 2014–2024 using monthly total precipitation derived from CHIRPS 2.0 and monthly mean temperature from Daymet v4. We generated time series graphs of these monthly values to identify the onset, duration, and peak of the monsoon season and to visualize interannual variability in precipitation and temperature (Ocampo-Marulanda et al., 2022). To evaluate dry monsoon years, we created annual bar charts of total precipitation, which allowed direct comparison of annual variation in monsoon intensity (Perera et al., 2017). Our analysis provided a temporal framework for identifying wet and dry monsoon years and for characterizing seasonal climate patterns relevant to vegetation dynamics in the study area.

2.3.2. Vegetation Seasonality

We analyzed vegetation seasonality using monthly-average NDVI and EVI from Terra MODIS for the period 2014–2024. We plotted these monthly time-series to visualize intra-annual greenness dynamics, taking advantage of EVI to avoid NDVI saturation in dense vegetation (Ehsanul et al., 2021). We identified the start of the growing season as the point when NDVI rose by approximately 20% above the winter baseline, following a threshold-based approach documented in phenological analyses (Berman et al*.,* 2020). We defined the peak of the growing season as the month with the maximum NDVI or EVI value. We identified the end of the growing season as the onset of a sustained downward trend in NDVI following peak greenness, a method commonly used in remote sensing phenology studies (Berman et al*.,* 2020). These phenological metrics guided the selection of Landsat 8 and Sentinel-2 acquisition dates, ensuring vegetation indices (NDVI, NDYI) were extracted during ecologically meaningful phases for aspen dynamics, such as the leaf senescence and leaf drop, so that it facilitates the classification of aspen in the study area.

2.3.3 Random Forest Classification Model (Aspen Classification)

Before running the RF classification, we assessed the spectral separability of vegetation classes using outputs from the vegetation seasonality analysis. We performed a bulk density analysis on NDVI standard deviation and October NDYI raster images representing autumn yellowing in October at the pixel level to assess how well these indices distinguished aspen from other land cover types, following approaches commonly used for evaluating class separability in spectral feature space (Foody, 2002). This confirmed that NDVI and NDYI can capture distinct seasonal signals for Aspen compared to Conifer, Shrub, and Grassland classes (Figure A1).

To prepare the training and testing data for the RF classification model, we applied a polygon leave-one-out sampling strategy combined with random stratified sampling. This ensured that training points were spatially independent and not clustered within the same polygon (Karasiak et al., 2022). We also sampled an equal number of points per class, which prevented the model from being biased toward classes with larger polygon areas (e.g., shrub or conifer) and ensured balanced class representation during model training (Shetty et al., 2021).

We stacked the predictor variables used for classification, including NDVI, NDYI, and MNDWI from Landsat 8 monthly composites and their interannual mean and standard deviation. We filtered out nonvegetative areas and limited the model to five vegetation classes: Aspen, Mixed Aspen, Conifer, Grassland, and Shrub. We trained the RF model using the randomForest package in RStudio with 75% of the points for training and 25% left for model testing (Araya et al., 2021). We generated confusion matrices for the classification map to assess classification accuracy and calculated per-class metrics (user's and producer's accuracy) along with overall accuracy. To quantify the influence of each predictor on model performance, we computed the Mean Decrease Gini index.

For the 2024 classification, we applied the same workflow for the RF model using HLS vegetation indices and selected spectral bands for aspen classification, while keeping the elevation data source identical to that

used in 2017. We imported the resulting 2017 and 2024 classification maps into ArcGIS Pro, where we calculated the total aspen forest area from the classified polygons. We used the two maps in the Classification Wizard tool in ArcGIS Pro to calculate zonal statistics and identify changes between class types from 2017–2024.

2.3.4 Aspen Health & Regeneration Assessment

Using the 2017 RF classification for aspen as a baseline, we evaluated changes in the health and extent of the Aspen class between 2017 and 2024 by computing ΔNDVI ($NDVI_{2024} - NDVI_{2017}$) derived from Landsat 8 at the pixel level. We used the magnitude of NDVI change to classify aspen condition into four categories: regrowth, mild stress, moderate decline, and tree loss, following the severity thresholds commonly applied in post-disturbance vegetation assessments (Priya & Vani, 2024). This approach provided a spatially explicit assessment of both decline and regeneration across the study area (Table A1).

To investigate potential drivers of aspen loss, we overlaid the boundaries of the Pipeline Fire (2022) perimeters with areas classified as tree loss. This comparison allowed us to identify whether recent fire activity corresponded with the spatial pattern of aspen decline. We also conducted a preliminary LiDAR-based assessment of post-fire aspen regeneration. We extracted available canopy height data from the relative height of 95% (rh_95) metric in the GEDI level 2A dataset (Figure A2). These data were obtained from available LiDAR products, clipped to the study area in R, and visualized to examine early structural recovery in burned forest patches. The available canopy height from March and April 2024 overlapped with the 2017 Aspen polygons from DePinte et al. (2018) and were separated into those inside and outside the Pipeline Fire (Figure A2). We refined the data occurring inside the burn boundary to only include areas that experienced a greater than 90% tree mortality according to the associated Rapid Assessment of Vegetation Condition After Wildfire (RAVG) dataset (USDA).

3. Results

3.1 Analysis of Results

3.1.1 Climate Assessment

Our analysis of precipitation and temperature showed annual and seasonal variability in precipitation and temperature through time and across the study area. Average monthly precipitation and temperature (Figure A3) show clear seasonal variability, whereas average yearly precipitation varies much more than average yearly temperature spatially (Figures A4 & A5). Precipitation remains low from January through May, reaching a minimum of ~3 mm in May, then rises sharply during the monsoon months of June through August, peaking at ~23 mm in August, before decreasing to ~5 mm by December. Temperature follows an opposite pattern, increasing from ~4 °C in January to a maximum of ~22 °C in July, and then gradually declining to ~6 °C in December. Annual average temperature seems to be more consistent across the study area between 2014-2023 (Figure A5). Annual monsoon precipitation fluctuates considerably from 2014-2024 (Figure A6). The wettest years are 2014, 2016, 2017, 2021, and 2022; each received more than 300 mm of rainfall, corresponding to strong monsoon seasons. The driest monsoons occurred in 2019 and 2020, when annual totals dropped below 150 mm, with 2020 representing the lowest precipitation year of the period. In 2024, total rainfall reached approximately 180 mm, higher than the driest years, but well below peak monsoon years.

3.1.2 Vegetation Seasonality

Figure A7 shows the monthly variation of NDVI and EVI across the study area from 2014-2024. Both indices exhibit a distinct seasonal pattern, with the growing season beginning in late April to early May, as NDVI rises from its winter baseline (~0.40) toward summer values. Peak vegetation occurs in July-August, with NDVI reaching ~0.76 and EVI peaking at ~0.86 in August. After the peak, both indices decline steadily, with NDVI decreasing to ~0.53 and EVI to ~0.72 by November, marking the end of the growing season. These seasonal markers (start, peak, and end of season) provide the temporal framework for selecting optimal dates for vegetation index calculations used in the RF classification and subsequent vegetation change analyses.

3.1.3 Random Forest Classification

For the first step, which assessed the ability of the chosen vegetation indices to distinguish between the Aspen and the other land cover classes in the study area, we conducted bulk density analyses of NDVI and NDYI. Bulk density analysis of NDVI standard deviation (Figure A8) demonstrated clear separability between classes. Aspen (yellow) shows higher NDVI standard deviation than Grassland (light green) and Conifer (dark green), which maintained a more consistent NDVI value through the year due to evergreen needle cover. The bulk density distributions for September NDYI (Figure A9) show that the Aspen class (yellow) exhibits higher NDYI values than the other vegetation classes. Grassland and Conifer (light and dark green) cluster at lower NDYI values, while Aspen displays a broader distribution extending toward higher values, reflecting the distinct autumn yellowing of aspen foliage. The bulk density analysis confirmed that NDVI standard deviation and seasonally informed NDYI layers clearly separate Aspen from other land cover classes, especially distinguishing deciduous aspen from evergreen conifers and low vegetation areas, such as grasslands. Based on this assessment, we included these indices as key predictor variables in our RF classification. Using this optimized predictor set, we generated the 2017 aspen classification map, which forms the basis for analyzing changes in aspen extent and condition over time.

Following the bulk density assessment, we trained the RF classification model and evaluated its performance in mapping Aspen and Mixed Aspen classes, while monitoring potential overfitting. The 2017 RF classification produced five vegetation classes, Aspen, Mixed Aspen, Conifer, Grassland, and Shrub, with an overall accuracy of 0.79 (Table 2). For Aspen, the model achieved a producer's accuracy (recall) of 0.754 and a user's accuracy (precision) of 0.736, yielding an F1-score of 0.745. However, Mixed Aspen showed lower accuracy (producer's = 0.678; user's = 0.727; F1 = 0.702), reflecting its transitional nature and high spectral overlap with neighboring vegetation types, which makes consistent classification more challenging.

Table 2
Random Forest Classification 2017 performance assessment

Class	Reference Data				
	Aspen	Mixed Aspen	Conifer	Grass	Shrub
User's Accuracy	0.754	0.678	0.898	0.771	0.856
Producer's Accuracy	0.736	0.727	0.835	0.771	0.886
F1-score	0.745	0.702	0.865	0.771	0.871

In 2024, (Table 3) the overall accuracy remained 0.79, but performance for Aspen improved. Aspen's user's accuracy increased to 0.80, while producer's accuracy stayed consistent at 0.74, resulting in a higher F1-score of 0.77. Mixed Aspen maintained a similar accuracy profile (producer's = 0.72; user's = 0.70; F1 = 0.71), remaining the most challenging class to map accurately due to its spectral blending with pure aspen and conifer stands. For more clarity about the confusion between classes in our random forest classification (2017 and 2024) see Tables A2 & A3 in the Appendix. Overall, Aspen classification improved slightly between 2017 and 2024, mainly through better precision, aided by using HLS vegetation indices and selected spectral bands in the 2024 model. Mixed Aspen remained consistently harder to classify due to its intermediate spectral characteristics and tendency to be confused with adjacent forest types.

Table 3
Random Forest Classification 2024 performance assessment

Class	Reference Data				
	Aspen	Mixed Aspen	Conifer	Grass	Shrub
User's Accuracy	0.80	0.70	0.78	0.80	0.89
Producer's Accuracy	0.74	0.72	0.85	0.85	0.79
F1-score	0.77	0.71	0.81	0.83	0.84

The variable importance analysis for the RF models identifies elevation as the most influential predictor in both 2017 (Figures A10) and 2024 (Figures A11), with a mean decrease in Gini score of nearly 200. In 2017, the next most important variables were NDVI in November and NDYI in October, highlighting the role of late-season phenology in distinguishing Aspen from Conifers. In 2024, using HLS data, NDVI in October and NDVI standard deviation ranked just below elevation. In both years, slope, aspect, and early-season bands had the lowest importance, indicating limited influence on Aspen classification compared to topography and autumn vegetation indices.

After confirming the RF model's performance statistically, we generated the final Aspen distribution map along with other land cover classes (Figure 2). In 2017 (Figure 2a), Aspen (blue) is concentrated in the northern and northcentral uplands, forming relatively continuous stands along higher elevations and north-facing slopes. Mixed Aspen/Conifer (yellow) occurs mainly as buffer zones surrounding core aspen stands, representing transitional areas with moderate conifer presence. In the southern portion of the study area, aspen is sparse and fragmented, occurring as small, isolated patches embedded within conifer-dominated forests. By 2024 (Figure 2b), the Aspen distribution shows both persistence in core high-elevation zones and notable changes along transitional edges. Many Aspen areas in the northern region remain intact, but portions have shifted to Mixed Aspen/Conifer, particularly along ecotonal boundaries. Some gains are also evident, with new Aspen patches emerging in areas previously classified as Grassland or Conifer, likely representing regeneration after disturbance events.

The change analysis quantified these transitions (Table A4). In 2017, Aspen covered 39.6 sq. miles, of which 47.1% persisted as Aspen in 2024. The remainder converted primarily to Mixed Aspen/Conifer (31.6%), Grassland (12.7%), Conifer (6.7%), or Shrub (2.0%). In turn, 31.3 sq. miles transitioned into Aspen from other classes, mainly from Mixed Aspen/Conifer (10.8 sq. miles), Conifer (10.4 sq. miles), and Grassland (9.8 sq. miles), shown in Table A5. Although total mapped aspen increased to 50.9 sq miles in 2024 (a net gain of 11.3 sq miles), the total forested area also expanded during this period. As a result, aspen's proportion of total forest cover declined from 15.5% in 2017 to 13.6% in 2024. This pattern suggests that while aspen coverage grew, other vegetation types may have grown at a faster rate or were left out of the 2017 classification due to low quality Landsat 8 imagery.

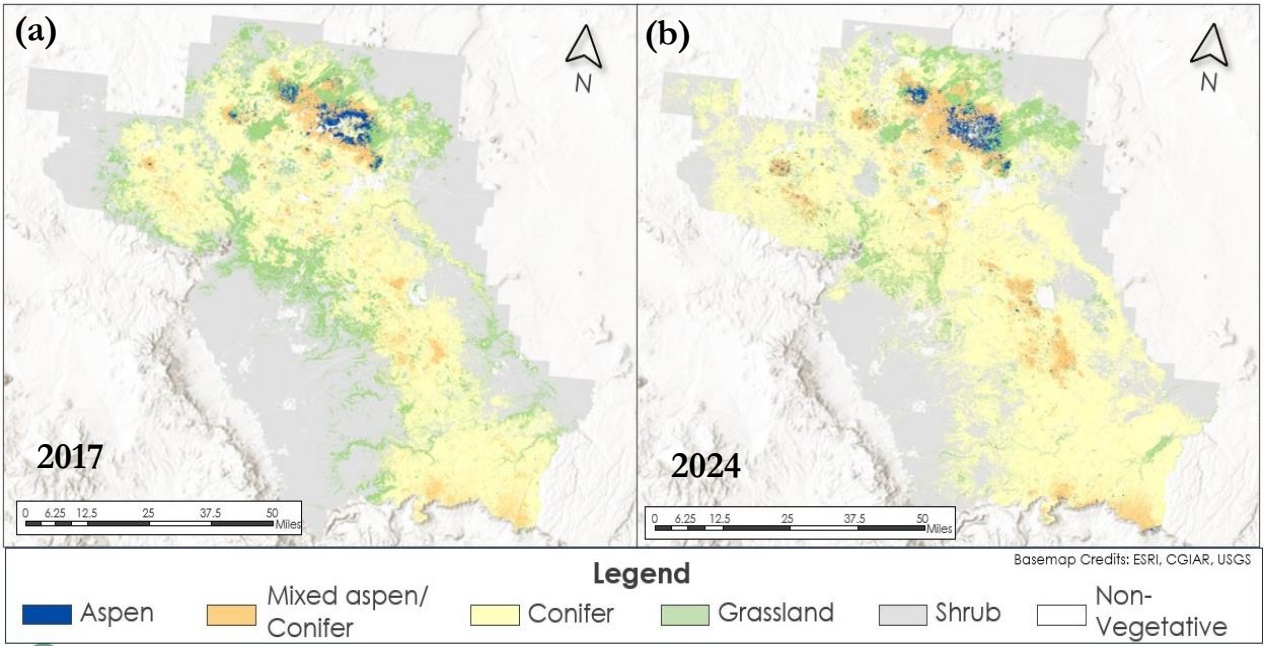

Basemap Credits: Esri, NASA, NGA, USGS, TomTom, Garmin, FAO, NOAA

Figure 2 a) Random Forest classification for 2017. This prediction was generated using the full model with all the input variables. b) Random Forest classification for 2024. This prediction was generated using the full model with all the input variables.

3.1.4 Aspen Health Assessment: Wildfire Case Studies

After calculating the NDVI difference between 2017 and 2024, we generated the NDVI change map to evaluate aspen forest condition (Figure A12). The analysis revealed a net NDVI decrease over approximately 24.8 sq. miles, representing 10.4% of the total forested area, indicating areas of aspen decline. Across the study area, 126 sq. miles showed NDVI increase (regrowth), 85 sq. miles had mild stress, and 9 sq. miles experienced NDVI decrease (tree loss). Notable areas of NDVI loss were concentrated within the perimeters of the Museum Fire (2019) and Pipeline Fire (2022), while additional clusters of decline coincided with known forest clear-cutting zones. This pattern highlights the combined influence of recent wildfires and timber harvests on aspen canopy loss, while also delineating localized areas of regrowth that provide opportunities for monitoring potential regeneration.

Figure A13 shows the median value of rh_95 (a proxy for canopy height) for GEDI points of aspen within the Pipeline burn scar and aspens outside of the Pipeline burn scar in March and April of 2024. The Mann-Whitney U test shows a significant difference (p-value < 0.005) between the canopy heights of aspen within the Pipeline Fire and outside of it. The median value of the aspen regeneration (37 feet) was lower than aspen unaffected by the wildfire (53 feet) (Figure 3). The number of available GEDI shots was limited for the aspen regeneration class and likely includes the dead trunks of other burned trees skewing the overall height to be higher than we would expect for areas of regeneration. The results point to potential aspen regeneration in areas severely burned by the Pipeline Fire but should be interpreted with uncertainty associated with limitations in canopy height data availability.

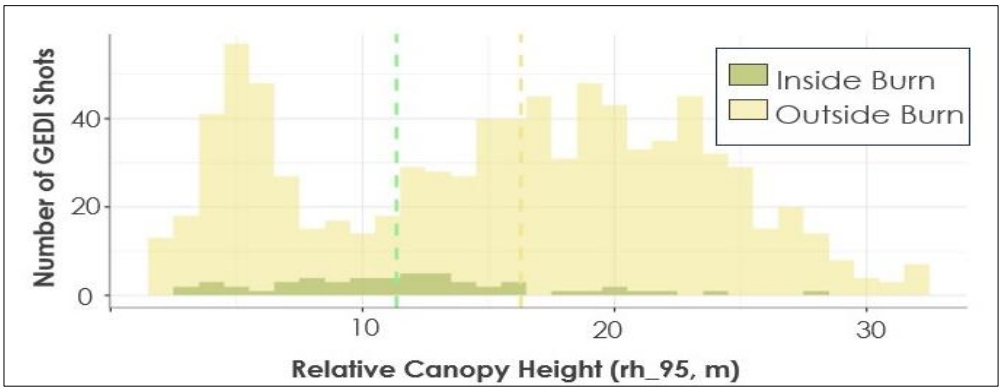

Figure 3. Histogram of the median canopy height for aspen inside vs. outside of the areas with high tree mortality from the Pipeline Fire. The median canopy height of each group is noted with a dashed line, 11.4 m (inside of the burn) and 16.3 m (outside of the burn).

3.2 Errors & Uncertainties

We initially performed a RF classification, which included the *moderate* conifer encroachment class from the partner-provided aerial data to generate aspen training points. This resulted in predicted aspen areas that exceeded the area of the 2017 NLCD deciduous class. Specifically, when we excluded *moderate* conifer encroachment polygons from generating aspen training points, the model detected far fewer aspen areas in the southeastern portion of our study area, which coincided with several aspen stands having moderate conifer encroachment (DePinte et al., 2018). This difference highlights the sensitivity of the RF classification model on the points chosen to represent different classes, such as the presence versus absence of aspen stands.

A notable limitation of this project was spatial resolution. Given higher resolution satellite imagery, the RF model and training datasets would be better able to identify smaller stands of aspen located within surrounding, dense conifer forest in the 30m tiles. Coarser spatial resolution leads to resampling of input indices that ultimately mix the spectral signature of aspen with other land classes that exist in proximity. Finer spatial resolution was available for more recent years, but it required more processing power and time than we had available for this project. Available GEDI footprints were inconsistent in coverage and timing for our study and were only available after 2018. For these reasons, this data processing level of GEDI data is missing much of the wildfire case study areas within the study area. Also, the temporal coverage for GEDI data often fell outside of the peak greenness season, making it difficult to incorporate biophysical vegetative metrics.

4. Conclusions

4.1 Interpretation of Results

Our analysis demonstrates that aspen dynamics in the study area are strongly influenced by climate variability, seasonal phenology, topography, and recent disturbances. The seasonality and bulk density analyses provided important pre-analysis steps for model development, helping identify the phenological windows and structural conditions most relevant for distinguishing Aspen from other vegetation types. As shown in the results of this study, it is feasible to use EOs to detect aspen in northern Arizona through a Random Forest classification. The 2017 and 2024 Random Forest classifications (both 79% accuracy) consistently mapped Aspen and Mixed Aspen, showing Aspen areas concentrated in high-elevation, north-facing slopes, while Mixed Aspen occurred mainly in transitional zones where conifer encroachment is most likely. Variable importance analysis confirmed that elevation and late-season NDVI and NDYI are the most influential predictors, underscoring the combined role of topography and autumn phenology in detecting and differentiating Aspen stands.

Between 2017 and 2024, aspen experienced a net canopy decline of 24.8 sq. miles (10.4%), with the largest losses corresponding to the Museum Fire (2019), Pipeline Fire (2022), and timber harvest areas. Much of this loss involved Aspen transitioning to Mixed Aspen/Conifer (31.6% of the 2017 aspen area), Grassland (12.7%), Conifer (6.7%), or Shrub (2%). Conversely, Aspen gained 31.3 sq. miles from other classes, including Mixed Aspen/Conifer (10.8 sq. miles), Conifer (10.4 sq. miles), and Grassland (9.8 sq. miles), indicating localized regeneration and recovery, particularly in post-disturbance landscapes. The change in aspen cover between 2017 and 2024 establishes a clear baseline for understanding aspen distribution and change over time, demonstrating that combining topographic context with seasonally optimized vegetation indices and informed by pre-analysis of seasonality and bulk density, effectively captures the phenological and structural differences critical for distinguishing deciduous aspen from other vegetation classes.

4.2 Feasibility & Partner Implementation

This project shows that the classification of locations with aspen trees in the study area is feasible using NASA EO data. The Random Forest model successfully mapped aspen distribution for 2017 and 2024, providing spatially explicit information on areas of persistence, decline, and regeneration, including those affected by wildfire and timber harvest. The workflow is fully reproducible and uses publicly available Landsat or HLS imagery, allowing it to be applied annually or after major disturbance events to track aspen distribution, assess regeneration, and identify areas requiring protection. This approach establishes a strong baseline for aspen detection and changes monitoring, while providing a scalable framework to support long-term, climate-sensitive forest management and conservation.

While the model is highly effective in identifying pure aspen stands, it is less precise in detecting mixed aspen/conifer areas, as it does not differentiate the degree of conifer encroachment. Nevertheless, classification maps and NDVI change products can be directly used to guide field verification, assess management outcomes, and prioritize restoration actions. Feasibility can be further enhanced by integrating higher-temporal-resolution imagery (e.g., from Sentinel-2 data) to improve NDYI values during September, when Landsat imagery is often limited by cloud cover, and by incorporating higher-spatial-resolution datasets to detect smaller aspen patches. Dividing the Mixed Aspen/Conifer class into low, medium, and high conifer encroachment levels would also provide more detailed management insights.

5. Acknowledgements

We would like to thank our partners (listed below) from USFS, NPS, AZ Department of Forestry and Fire Management, and NAU; our NASA DEVELOP Lead Jane Zugarek; our DEVELOP Project Coordinator Kaitlyn Lemon; and our Science Advisors Dr. Xia Cai, Dr. Paul Arellano, and Dr. Alexander Shenkin, who all contributed to the success of this project.

Project Partners:

- USFS, Coconino National Forest, Flagstaff Ranger District – **Mark Nabel**, **Andy Pigg**, **Christopher Curley**, **Jack Daugherty**, **Noah Bard**
- NPS, Wupatki, Sunset Crater Volcano, Walnut Canyon National Monuments – **Mark Szydlo**
- AZ Dept. of Forestry and Fire Management – **Aly McAlexander**
- Northern Arizona University School of Forestry – **Dr. Kristen Waring**
- USFS, Northern Research Station – **Dr. Connor Crouch**
  USFS, Southwestern Region, Arizona Zone Forest Health – **Amanda Grady**, **Nicholas Wilhelmi**
  USFS, Coconino National Forest, Mogollon Rim Ranger District – **Mary Price**, **Brett Miller**

Any opinions, findings, and conclusions or recommendations expressed in this material are those of the author(s) and do not necessarily reflect the views of the National Aeronautics and Space Administration.

This material is based upon work supported by NASA through contract 80LARC23FA024.

6. Glossary

CHIRPS – Climate Hazards Group Infrared Precipitation
Coconino N.F. – Coconino National Forest, a mountainous region of forested land located in Northern Arizona and in the jurisdiction of the federal U.S. Forest Service
CRS – Coordinate Reference System
CSV – Comma Separated Values
DEM – Digital Elevation Model
Earth observations or **EOs** – Satellites and sensors that collect information about the Earth's physical, chemical, and biological systems over space and time
EVI – Enhanced Vegetation Index
GEE – Google Earth Engine
GEDI – Global Ecosystem Dynamics Investigation
HDF – Hierarchical Data Format
HLS – Harmonized Landsat-Senitnel-2
LiDAR – Light Detection and Ranging
MNDWI – Modified Normalized Difference Water Index
MODIS – Moderate Resolution Imaging Spectroradiometer
NDVI – Normalized Difference Vegetation Index
NDYI – Normalized Difference Yellow Index
NLCD – National Land Cover Database
NPS – National Park Service
Oystershell scale – *Lepidosaphes ulmi,* an invasive scale insect present in North America as early as the 1700s. These insects attach to the trunks and branches of aspen trees and feed on the sap, thereby reducing the moisture available to the tree and increasing its susceptibility to pathogens, and even killing the tree.
RAVG – Rapid Assessment of Vegetation Condition After Wildfire
RF – Random Forest
SRTM – Shuttle Radar Topography Mission
USDA – United States Department of Agriculture
USFS – United States Forest Service

7. References

Araya, S. N., Fryjoff-Hung, A., Anderson, A., Viers, J. H., & Ghezzehei, T. A. (2021). Advances in soil moisture retrieval from multispectral remote sensing using unoccupied aircraft systems and machine learning techniques. Hydrology and Earth System Sciences, 25(5), 2739–2758. https://doi.org/10.5194/hess-25-2739-2021

Ehsanul, B., Nusrat, J. N., & Bishal, R. (2021). Association of vegetation indices with atmospheric & biological factors using MODIS time series products. *Environmental Challenges, 5*, 100376. https://doi.org/10.1016/j.envc.2021.100376

Berman, E. E., Graves, T. A., Mikle, N. L., Merkle, J. A., Johnston, A. N., & Chong, G. W. (2020). Comparative quality and trend of remotely sensed phenology and productivity metrics across the Western United States. *Remote Sensing, 12*(16), 2538. https://doi.org/10.3390/rs12162538

Climate Hazards Group. (2015). *CHIRPS Version 2.0: Climate Hazards Group InfraRed Precipitation with Station Data* [dataset]. University of California, Santa Barbara. https://data.chc.ucsb.edu/products/CHIRPS-2.0/

Cook, M., Chapman, T., Hart, S., Paudel, A., & Balch, J. (2024). Mapping quaking aspen using seasonal Sentinel-1 and Sentinel-2 composite imagery across the Southern Rockies, USA. *Remote Sensing*, 16(9), 1619. https://doi.org/10.3390/rs16091619

Crouch, C. D., Grady, A. M., Wilhelmi, N. P., Hofstetter, R. W., DePinte, D. E., & Waring, K. M. (2021). Oystershell scale: An emerging invasive threat to aspen in the southwestern US. *Biological Invasions, 23*(9), 2893–2912. https://doi.org/10.1007/s10530-021-02545-0

Crouch, C. D., Wilhelmi, N. P., Rogers, P. C., Moore, M. M., & Waring, K. M. (2025). Sustainability and drivers of *Populus tremuloides* regeneration and recruitment near the southwestern edge of its range. *Forestry: An International Journal of Forest Research, 98*(2), 148–166. https://doi.org/10.1093/forestry/cpae018

DePinte, D. E. (2018). *Aspen Mapping Project: Williams Ranger District, Kaibab National Forest and Flagstaff, Mogollon Rim Ranger Districts, Coconino National Forest*. U.S. Forest Service, Southwestern Region, Forest Health Protection, Arizona Zone.

Didan, K. (2015). *MOD13Q1 MODIS/Terra Vegetation Indices 16-Day L3 Global 250m SIN Grid, Version 6* [dataset]. NASA EOSDIS Land Processes DAAC. https://doi.org/10.5067/MODIS/MOD13Q1.006

Dubayah, R., Blair, J. B., Hofton, M. A., Tang, H., Duncanson, L., Hancock, S. & Armston, J. (2020). *GEDI Level 2A and 2B Canopy Height and Vertical Structure Metrics, Version 2* [dataset]. NASA ORNL DAAC. https://doi.org/10.3334/ORNLDAAC/2056

Earth Resources Observation and Science (EROS) Center. (2014). *NASA Shuttle Radar Topography Mission (SRTM) 1 Arc-Second Global* [dataset]. U.S. Geological Survey. https://doi.org/10.5066/F7PR7TFT

Earth Resources Observation and Science (EROS) Center. (2020). *Landsat 8–9 Operational Land Imager / Thermal Infrared Sensor Level-2, Collection 2* [dataset]. U.S. Geological Survey. https://doi.org/10.5066/P9OGBGM6

Foody, G. M. (2002). Status of land cover classification accuracy assessment. *Remote Sensing of Environment*, *80*(1), 185–201. https://doi.org/10.1016/s0034-4257(01)00295-4

Forestry. (2023). *Coconino National Forest*. Forestry.com. https://forestry.com/national-forests/coconino-national-forest/

Funk, C. C., Peterson, P. J., Landsfeld, M. F., Pedreros, D. H., Verdin, J. P., Rowland, J. D., Romero, B. E., Husak, G. J., Michaelsen, J. C., & Verdin, A. P. (2015). The climate hazards infrared precipitation with stations—a new environmental record for monitoring extremes. *Scientific Data, 2*, 150066. https://doi.org/10.1038/sdata.2015.66

Gorelick, N., Hancher, M., Dixon, M., Ilyushchenko, S., Thau, D., & Moore, R. (2017). Google Earth Engine: Planetary-scale geospatial analysis for everyone. *Remote Sensing of Environment, 202*, 18–27. https://doi.org/10.1016/j.rse.2017.06.031

Grigorieva, O., Brovkina, O., & Saidov, A. (2020). An original method for tree species classification using multitemporal multispectral and hyperspectral satellite data. *Silva Fennica, 54*(2). https://www.silvafennica.fi/article/10143/author/19113

Hamilton, R., Megown, K., DiBenedetto, J., Bartos, D., & Mileck, A. (2009). *Assessing Aspen Using Remote Sensing*. U.S. Forest Service. https://www.fs.usda.gov/rm/pubs_other/rmrs_2009_hamilton_r001.pdf

Karasiak, N., Dejoux, J.-F., Monteil, C., & Sheeren, D. (2022). Spatial dependence between training and test sets: Another pitfall of classification accuracy assessment in remote sensing. *Machine Learning*, 111(4), 2715–2740. https://doi.org/10.1007/s10994-021-05972-1

Kriegler, F., Malila, W., Nalepka, R., & Richardson, W. (1969). Preprocessing transformations and their effect on multispectral recognition. Proceedings of the 6th International Symposium on Remote Sensing of Environment. Ann Arbor, MI: University of Michigan, 97-131.

Masek, J., Ju, J., Roger, J.-C., Skakun, S., Vermote, E., Claverie, M., Dungan, J., Yin, Z., Freitag, B., & Justice, C. (2021). HLS Sentinel-2 Multi-spectral Instrument Surface Reflectance Daily Global 30m v2.0 [data set]. NASA Land Processes Distributed Active Archive Center. https://doi.org/10.5067/HLS/HLSS30.002 Date Accessed: 2025-08-05

Ocampo-Marulanda, C., López-Barriga, J. S., Martínez-Romero, A., & Díaz-Varela, E. (2022). A spatiotemporal assessment of the high-resolution Climate Hazards InfraRed Precipitation with Station data (CHIRPS). *Ain Shams Engineering Journal, 13*(5), 101739. https://doi.org/10.1016/j.asej.2022.101739

Oukrop, C., Evans, D., Bartos, D., Ramsey, R., & Ryel, R. (2011). *Moderate-Scale Mapping Methods of Aspen Stand Types: A Case Study for Cedar Mountain in Southern Utah*. United States Department of Agriculture, Forest Service, Rocky Mountain Research Station. https://www.fs.usda.gov/rm/pubs/rmrs_gtr259.pdf

Perera, E. N. C., Jayawardana, D. T., & Jayasinghe, P. (2017). A rainfall intensity-duration threshold for mass movement in Badulla, Sri Lanka. *Journal of Geoscience and Environment Protection, 5*(12), 135–152. https://doi.org/10.4236/gep.2017.512010

Priya, R. S. & Vani, K. (2024). Vegetation change detection and recovery assessment based on post-fire satellite imagery using deep learning. *Scientific Reports, 14*, 12611. https://doi.org/10.1038/s41598-024-63047-2

Sankey, T. T. (2011). Decadal-scale aspen changes: Evidence in remote sensing and tree ring data. *Applied Vegetation Science, 15*(1). https://doi.org/10.1111/j.1654-109X.2011.01141.x

Shaw, J. D., Menlove, J., Witt, C., Morgan, T. A., Amacher, M. C., Goeking, S. A., & Werstak, C. E. (2018). *Arizona's forest resources, 2001–2014*. U.S. Department of Agriculture, Forest Service, Rocky Mountain Research Station. https://doi.org/10.2737/RMRS-RB-25

Shetty, S., Gupta, P. K., Belgiu, M., & Srivastav, S. K. (2021). Assessing the effect of training sampling design on the performance of machine learning classifiers for land cover mapping using multi-temporal remote sensing data and Google Earth Engine. *Remote Sensing, 13*(8), 1433. https://doi.org/10.3390/rs13081433

Stoddard, M. T., Rodman, K. C., Crouch, C. D., Huffman, D. W., Fulé, P. Z., Waring, K. M., & Moore, M. M. (2024). Multi-decadal aspen dynamics show recruitment bottleneck across complex mountain community. *Forest Ecology and Management, 572*. https://doi.org/10.1016/j.foreco.2024.122326

Sulik, J. J., & Long, D. S. (2016). Spectral considerations for modeling yield of canola. *Remote Sensing of Environment, 184*, 161–174. https://doi.org/10.1016/j.rse.2016.06.016

Thornton, M. M., Thornton, P. E., Mayer, B. W., Wei, Y., Devarakonda, R., Vose, R. S., & Cook, R. B. (2021). *Daymet: Daily Surface Weather Data on a 1-km Grid for North America, Version 4* [dataset]. NASA Oak Ridge National Laboratory Distributed Active Archive Center (ORNL DAAC). https://doi.org/10.3334/ORNLDAAC/2129

Troshin, D., Fayzulin, M., & Mirin, D. (2025). Spatial and temporal classification and prediction of aspen probability in boreal forests using machine learning algorithms. *Environmental Monitoring and Assessment, 197*(5), 527. https://doi.org/10.1007/s10661-025-13985-9

United States Department of Agriculture. (2025). *Coconino National Forest | About the Area | Forest Service*. http://www.fs.usda.gov/r03/coconino/about-area

United States Department of Agriculture. (2022). *RAVG Initial assessment of the 2022 PIPELINE fire (Event ID AZ3527011166620220612)*. Forest Service. https://burnseverity.cr.usgs.gov/ravg/

Walz, J. H., & Weber, K. T. (2021). Identifying actively growing vegetation using NDVI threshold values. *NASA Idaho Space Grant Consortium*. Retrieved from https://giscenter.isu.edu/Research/Techpg/NASA_ISGC/pdf/AGV_threshold_final.pdf

Xu, H. (2006). Modification of normalized difference water index (NDWI) to enhance open water features in remotely sensed imagery. *International Journal of Remote Sensing, 27*(14), 3025–3033. https://doi.org/10.1080/01431160600589179

8. Appendix A

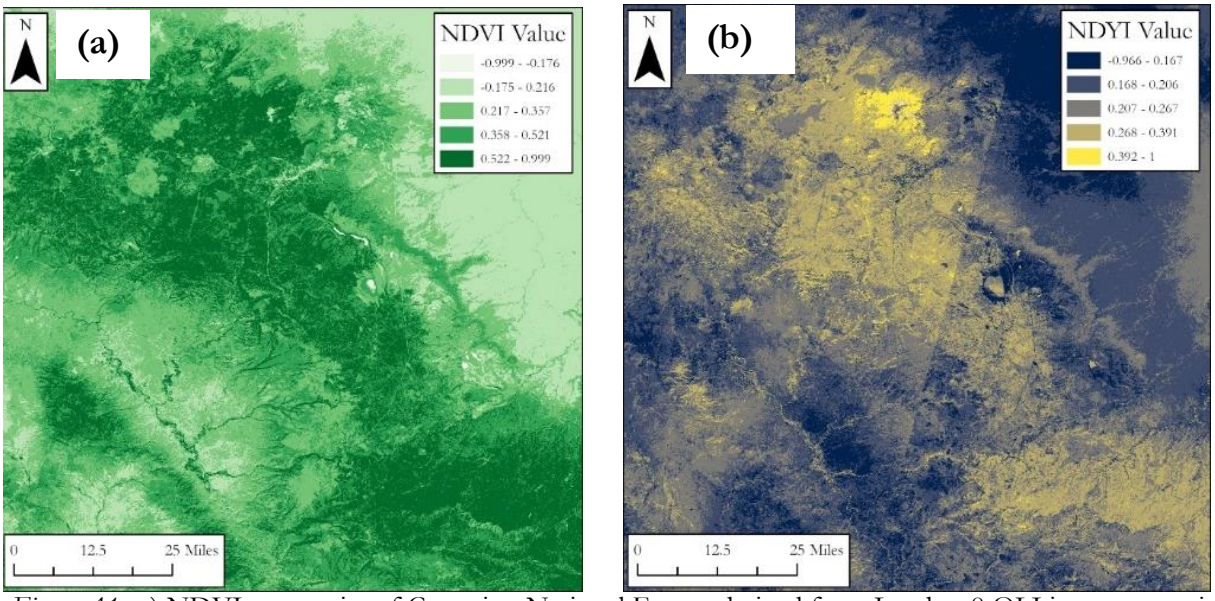

Figure A1. a) NDVI composite of Coconino National Forest, derived from Landsat 8 OLI imagery acquired in October 2017. Darker green tones represent higher NDVI values, indicating denser or healthier vegetation, while lighter greens reflect areas of lower vegetation density or reflectance. b) NDYI composite of Coconino National Forest, derived from Landsat 8 OLI imagery acquired in October 2017. Brighter yellow areas indicate higher NDYI values, typically associated with deciduous vegetation and seasonal phenological changes, while darker tones correspond to evergreen cover, shadows, or sparse vegetation. (Source: Landsat 8 OLI, 2017)

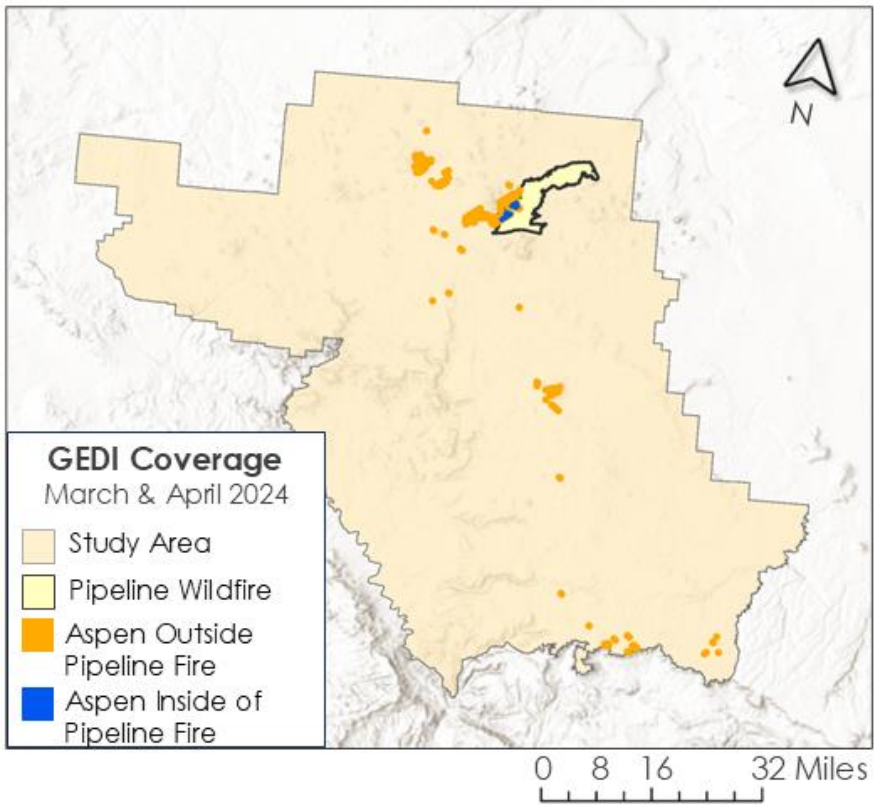

Figure A2. Map of GEDI Level 2A from March and April 2024 to get canopy height (rh_95) for 2024 aspen occurring in areas with > 90% tree mortality in the Pipeline Fire (2022) and for aspen in the study area outside of the Pipeline burn boundary.

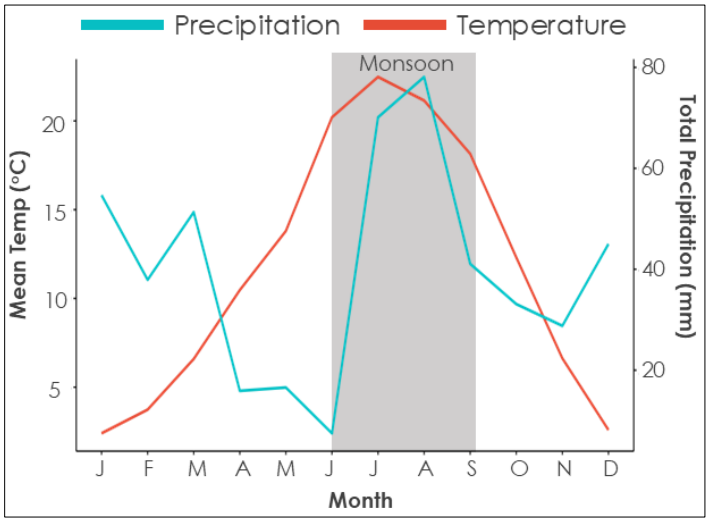

Figure A3. Line plot showing the monthly variability of mean temperature (red) and total precipitation (blue) for each month, averaged across 2014-2023.

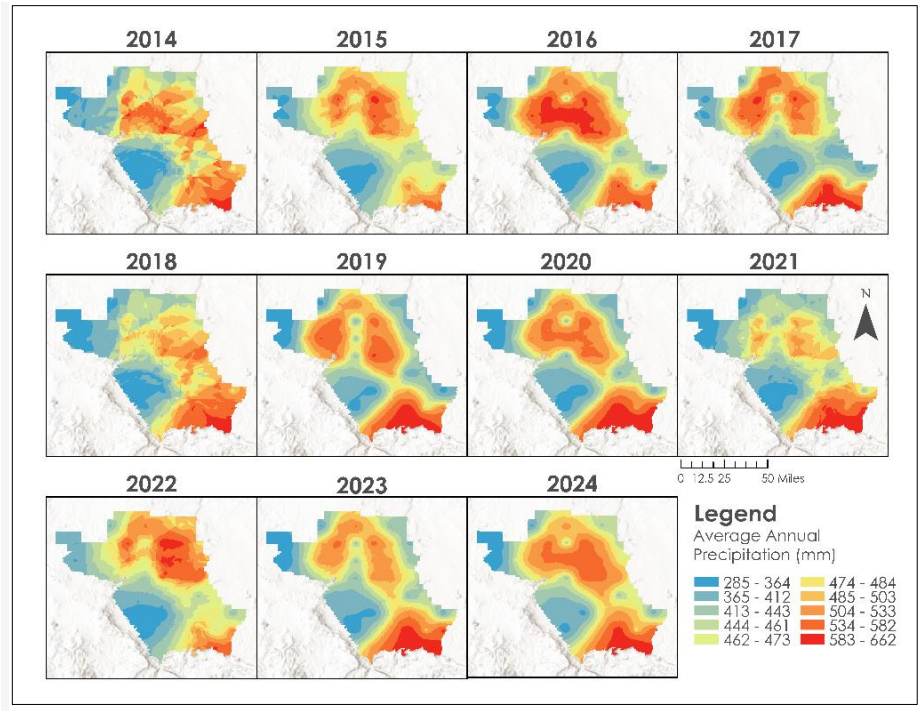

Figure A4. Spatial distribution of average annual precipitation for years 2014 to 2024. Precipitation data is from CHIRPS and interpolated using the Empirical Bayesian kriging (EBK) method.

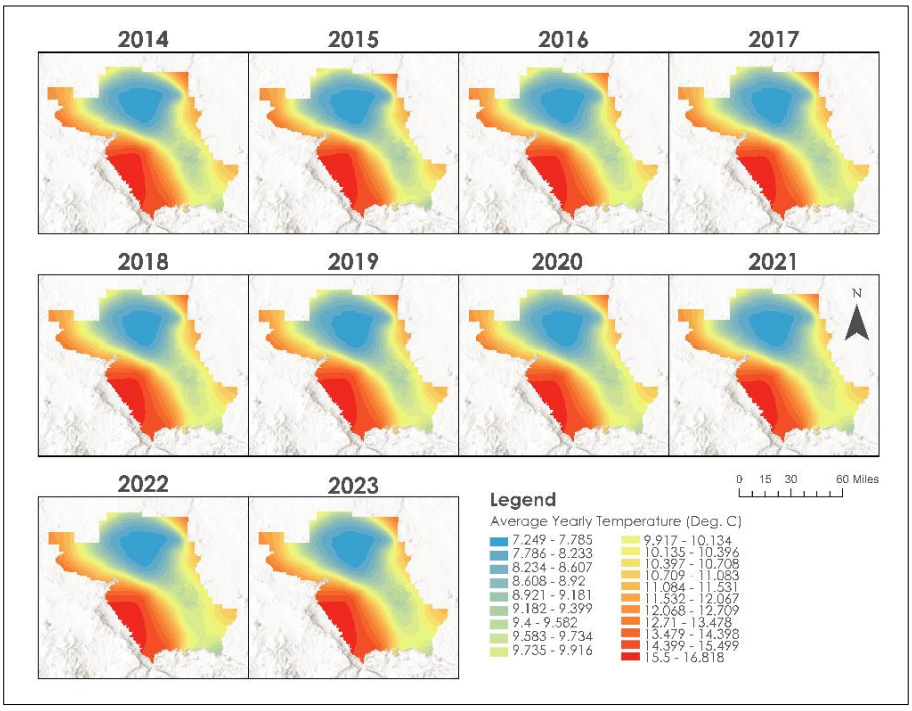

Figure A5. Spatial distribution of average yearly temperature for years 2014 to 2024. Temperature data is from DayMet and interpolated using the Empirical Bayesian kriging (EBK) method.

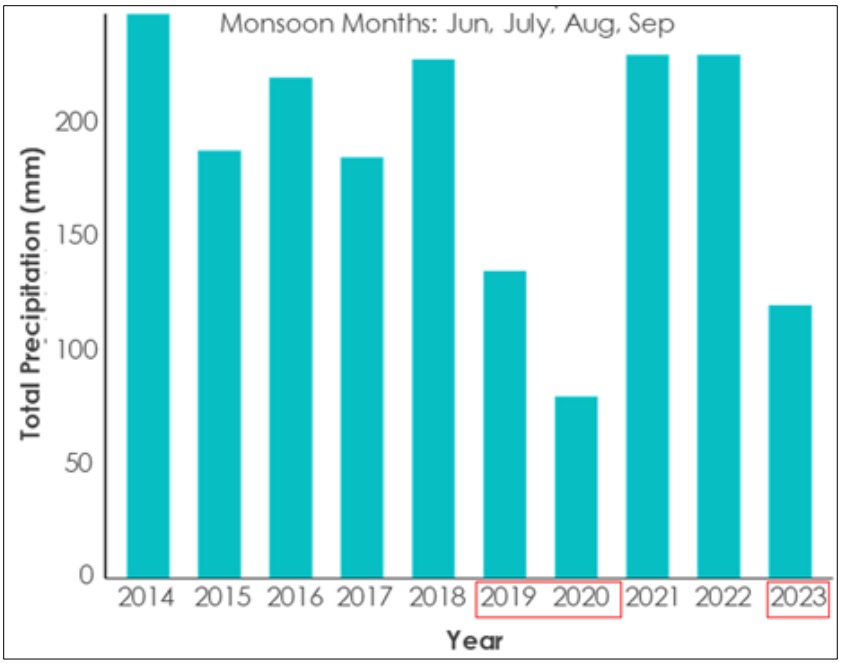

Figure A6. Bar chart of monsoon precipitation (totaled from June, July, August, and September) for the study area by year from 2014 to 2023. Years that fell below the average rainfall for this period are boxed in red.

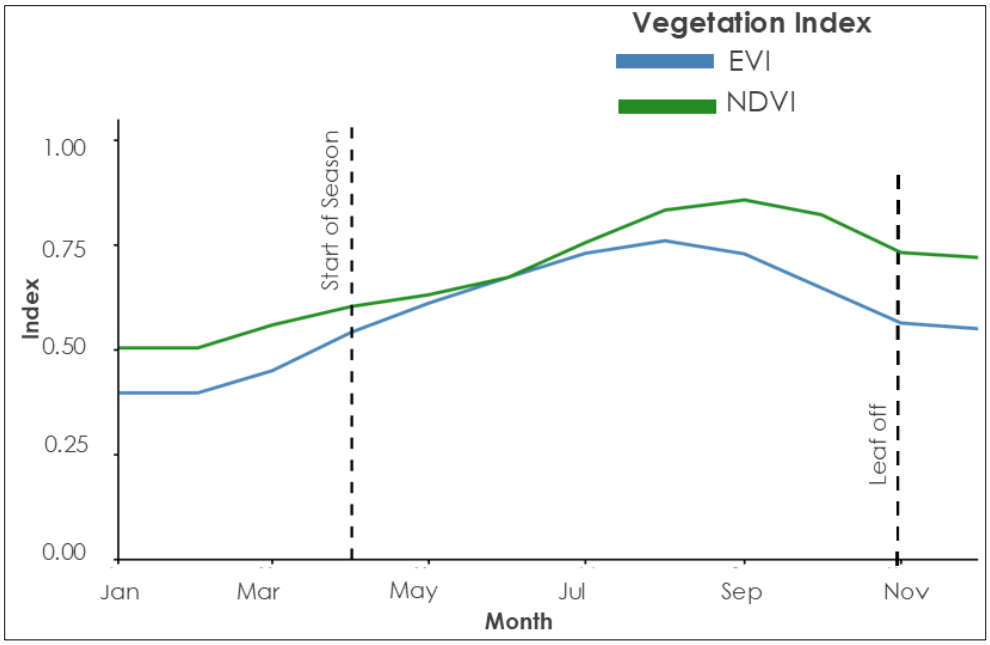

Figure A7. Line graph of average monthly NDVI and EVI calculated from 2014-2024 averaged across the study region. Data from Terra MODIS Vegetation Indices product.

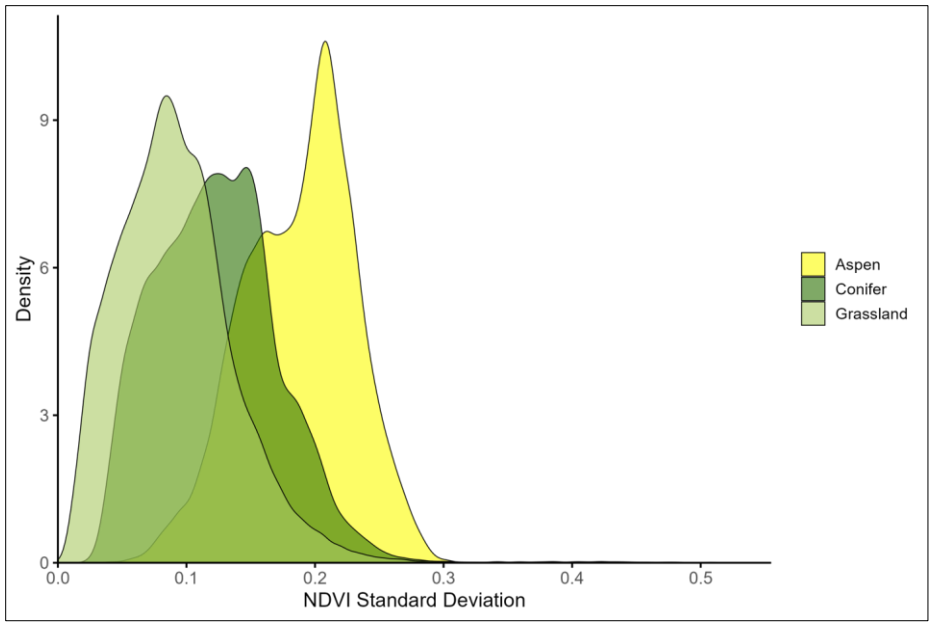

Figure A8. Pixel bulk density distribution of standard deviation of NDVI calculated from monthly composite imagery for 2017, separated by Aspen, Conifer, and Grassland classes as determined by overlap with training polygons of the same class.

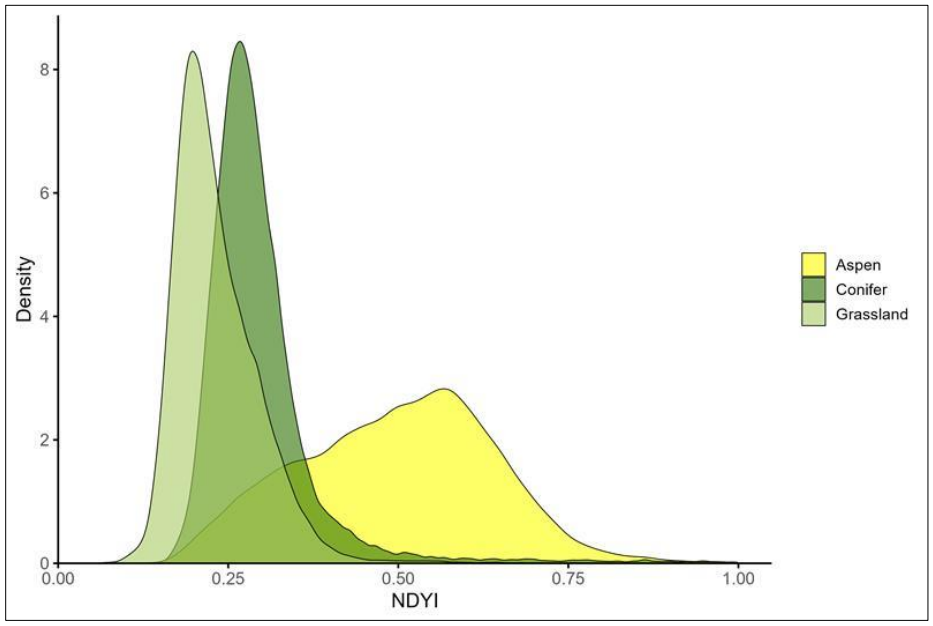

Figure A9. Pixel bulk density distribution of NDYI for September 2017, separated by Aspen, Conifer, and Grassland classes as determined by overlap with training polygons of the same class. The aspen distribution has a higher NDYI value and a wider range than Conifer and Grassland classes.

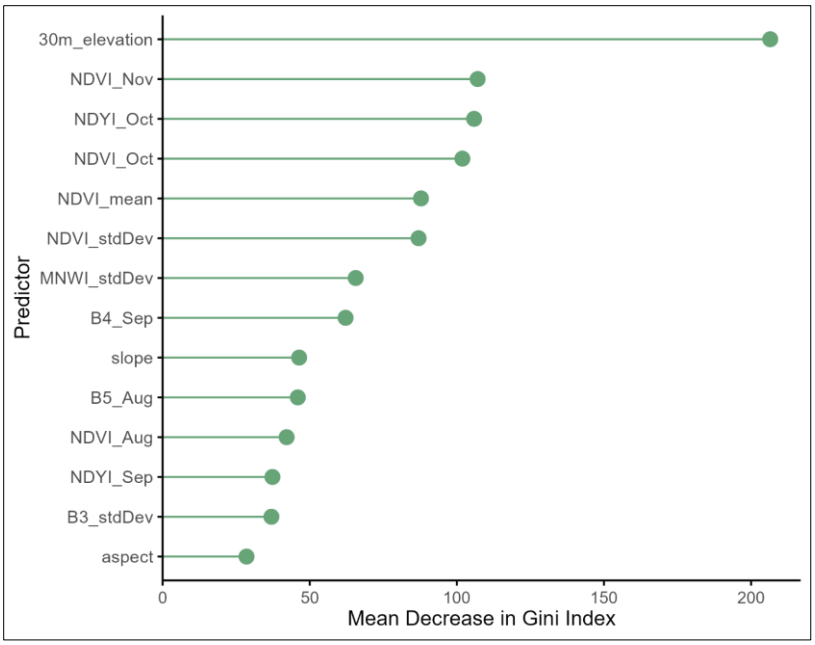

Figure A10. Variable importance for 2017 classification determined by mean decrease in Gini index.

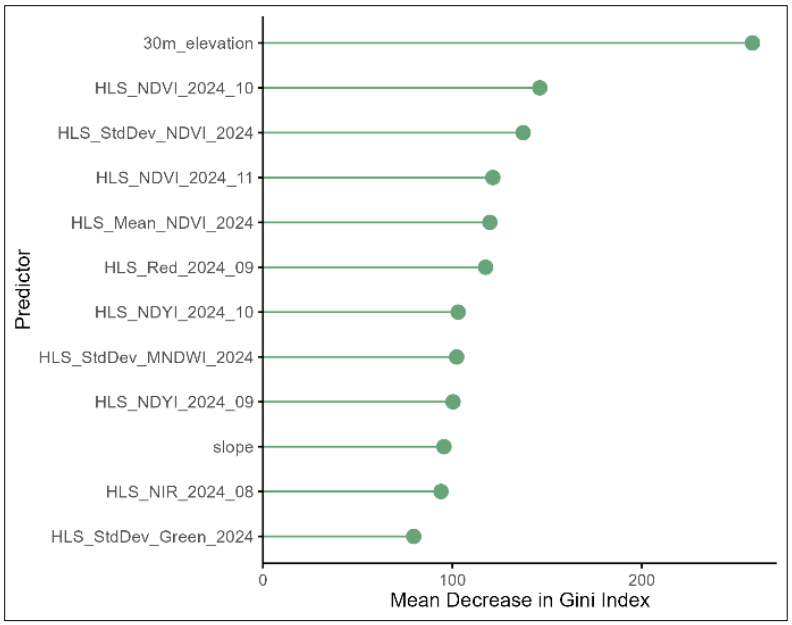

Figure A11. Variable importance for 2024 classification determined by mean decrease in Gini index.

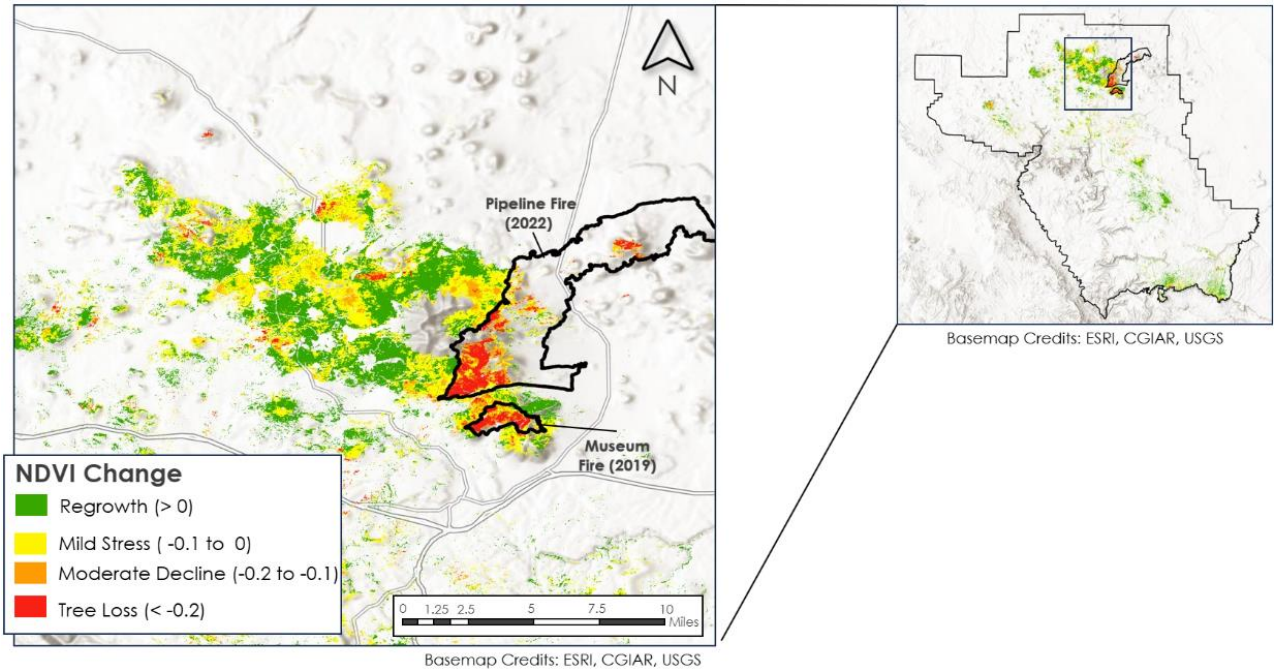

Figure A12. Change in NDVI between 2017 and 2024 for areas identified as aspen in 2017 random forest classification.

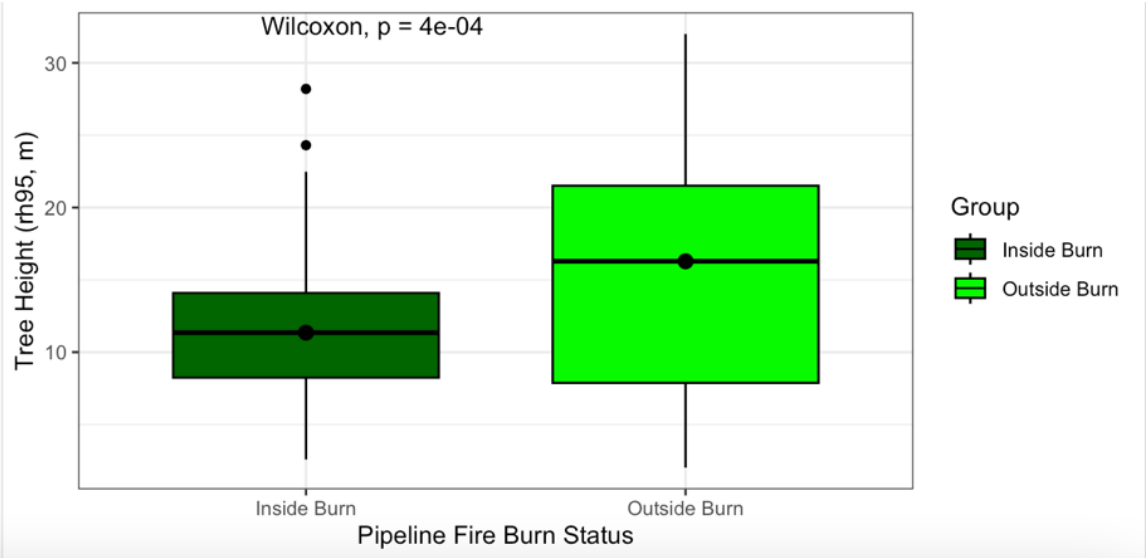

Figure A13. Box and whisker plot of the median canopy height for aspen inside vs. outside of the areas with high tree mortality from the Pipeline Fire. The Wilcoxon signed-rank sum test with continuity correction results: w = 15537, p-value = 0.0004046.

Table A1. Parameters, as defined in *Walz & Weber, 2021*, for interpretation of NDVI change on vegetation health.

NDVI Change	Interpretation
> 0	Vegetation increase/ regrowth
0 to -0.1	Normal variation, mild stress
-0.1 to -0.2	Moderate decline — *may* indicate early stress
≤ -0.2	**Reliable indicator of canopy/tree loss**
≤ -0.25 / -0.3	Strong canopy loss (e.g., drought, fire, dieback)

Table A2. Confusion matrix for random forest 2017 classification.

Class	**Reference Data**				
	Aspen	Mixed Aspen	Conifer	Grass	Shrub
Aspen	89	22	1	7	2
Mixed Aspen	21	80	9	0	0
Conifer	2	10	106	7	2
Grass	6	6	2	91	13
Shrub	0	0	0	13	101
User's Accuracy	0.754	0.678	0.898	0.771	0.856
Producer's Accuracy	0.736	0.727	0.835	0.771	0.886
F1-score	0.745	0.702	0.865	0.771	0.871

Table A3. Confusion matrix for random forest 2024 classification.

Class	**Reference Data**				
	Aspen	Mixed Aspen	Conifer	Grass	Shrub
Aspen	91	23	2	6	1
Mixed Aspen	19	88	13	2	1
Conifer	0	12	105	2	4
Grass	2	3	7	105	6
Shrub	2	0	8	16	97
User's Accuracy	0.80	0.70	0.78	0.80	0.89
Producer's Accuracy	0.74	0.72	0.85	0.85	0.79
F1-score	0.77	0.71	0.81	0.83	0.84

Table A4. Change in area of classes (in mi2) between 2017 and 2024 based on random forest classifications.

	2017 Random Forest Classification	2024 Random Forest Classification	Change in Area (2024–2017)
Aspen	41	53	+12
Mixed Conifer/Aspen	195	255	+60
Conifer	1292	1958	+666
Grassland	555	312	-243
Shrub	1837	1337	-500

Table A5. Total area in the conversion of land classes between the 2017 and 2024 classifications. Rows are shaded by class type in 2024.

Change in class from 2017to 2024	Area (sq.miles)
Aspen (No change)	18.64
Aspen to Conifers	2.64
Aspen to Grassland	5.02
Aspen to Mixed Aspen/ conifer	12.49
Aspen to Shrub	0.79
Conifers (No change)	1100.84
Conifers to Aspen	10.45
Conifer to Grassland	49.42
Conifer to Mixed Aspen/ conifer	106.76
Conifers to Shrubs	12.75
Grassland (No change)	153.97
Grassland to Aspen	9.84
Grassland to Conifers	298.17
Grassland to Mixed Aspen/ conifer	12.89
Grassland to Shrub	65.82
Mixed Aspen/conifer (No change)	115.80
Mixed Aspen/conifer to Aspen	10.84
Mixed Aspen/ conifer to Conifers	58.59
Mixed Aspen/ conifer to Grassland	6.83
Mixed Aspen/ conifer to Shrub	0.6
Shrub (No change)	1251.97
Shrub to Aspen	0.17
Shrub to Conifers	473.44
Shrub to Grassland	92.68
Shrub to Mixed Aspen/ conifer	0.38